Nonlinear Dyn (2008) 53: 89–106
DOI 10.1007/s11071-007-9298-y

ORIGINAL PAPER

Nonlinear vibration of shallow cables with semiactive tuned mass damper

Fabio Casciati · Filippo Ubertini

Received: 18 December 2006 / Accepted: 23 August 2007 / Published online: 29 September 2007

Abstract The nonlinear vibration of shallow cables, equipped with a semiactive control device is considered in this paper. The control device is represented by a tuned mass damper with a variable out-of-plane inclination. A suitable control algorithm is designed in order to regulate the inclination of the device and to dampen the spatial cable vibrations. Numerical simulations are conducted under free spatial oscillations through a nonlinear finite element model, solved in two different computational environments. A harmonic analysis, in the region of the primary resonance, is also performed through a control-oriented nonlinear Galerkin model, including detuning effects due to the cable slackening.

Keywords Bifurcations · Galerkin approach · Numerical simulations · Structural cables · Tuned mass damper

Abbreviations

x, y, z, s	Reference axes and curvilinear abscissa
t, τ, χ	Time, normalized time and normalized abscissa
C_0, C_1	Cable static and varied configurations
u, v, w	Cable displacements functions
d, l	Cable sag and cable span
E, S	Elastic modulus and cross section
H	Cable horizontal reaction
μ, c_v, c_w	Mass and damping coefficients per unit length
p_y, p_z	Distributed in-plane and out-of-plane loads
$\bar{e}$	Constant Lagrangian measure of strain
ω_{iv}, ω_{iw}	In-plane and out-of-plane natural circular frequencies
p_{iv}, p_{iw}, Ω	Normalized modal loads and circular frequency
q_i^v, q_i^w	In-plane and out-of-plane modal coordinates
n_v, n_w	Number of in-plane and out-of-plane modes retained in the Galerkin models
a_{0ij}, a_{1i}, a_{2j}	Coefficients of the Galerkin models
$a_{3i}, b_{1j}, b_{2ij}, b_{3k}$	Coefficients of the Galerkin models
ξ_i^v, ξ_i^w	Damping coefficients in the Galerkin models
$\mathbf{U}, \mathbf{\Delta U}$	Vectors of nodal displacements in FEM models
$\sigma, \tilde{\sigma}$	Error and error tolerance in the FEM procedure
n	Number of unconstrained nodes in the FEM models
m, c, k	Mass, damping coefficient and stiffness of the TMD

F. Casciati · F. Ubertini (✉)
Department of Structural Mechanics, University of Pavia,
Via Ferrata 1, 27100 Pavia, Italy
e-mail: filippo.ubertini@unipv.it

ξ_d, ω_d	Damping ratio and circular frequency of the TMD
ι, ω	Imaginary unit and complex circular frequency
β	Fundamental complex eigenvalue
ω_0	First in-plane circular frequency of a cable without sag
α, ε	In-plane and out-of-plane TMD inclinations
x_0, r	Position and local axis of the TMD
R	Length of the TMD
η_0, V	Cable and TMD displacements
ξ, ζ	Control forces
γ	Mass ratio of the cable-TMD system
$\tilde{\alpha}$	Scalar parameter of the time integration scheme
$g_{\varepsilon 1}$, $g_{\varepsilon 2}$	Control gains
ψ, ν, λ^2	Nondimensional cable parameters
f_i^v, f_i^w	Cable natural frequencies
v_m, w_m	Cable mid-span displacements
v_{1q}, w_{3q}	Cable observed displacements
α_C, β_C	Rayleigh damping matrix parameters
$\bar{q}_1^w$, $\bar{q}_2^w$	Estimates of the first two out-of-plane modal amplitudes

1 Introduction

Steel cables are structural elements adopted in several engineering applications, such as suspension and cable-stayed bridges, off-shore platforms, transmission power lines and other cable-supported structures. Environmental excitations, such as wind, bridge traffic, rain-wind interaction, etc., may result in large amplitude cable vibrations, since the cables show modest damping properties. Vibrations can also result in cable or connection failures due to fatigue, as well as in a damaging of the corrosion protection system. Such vibrations mainly involve the first in-plane and out-of-plane modes. Nevertheless, modal interactions and coupling phenomena may also involve higher order modes, due to quadratic and cubic nonlinearities in the equations of motion. These aspects were widely investigated in the literature and were summarized in two recent review articles by Rega [1, 2]. The former [1] is mainly focused on cable dynamics modeling, while the latter [2] deals with deterministic nonlinear phenomena that arise in the cable motion. The well-known bifurcation of the first in-plane mode into a bi-modal spatial oscillation was analyzed in the paper by Larsen and Nielsen [3], while multi-modal interactions under parametric external excitation were investigated by Perkins [4]. When internal resonances occur, those nonlinear phenomena are even enhanced, as pointed out by Nayfeh et al. [5] and by Benedettini et al. [6].

The behavior of an arbitrarily sagged cable can be modeled as a prestressed mono-dimensional linearly elastic continuum with no flexural, torsional or shear stiffness, as early outlined by Luongo et al. [7]. Different elastic cable theories were developed referring to either small-sag or large-sag cables. In the former case, the analytical continuum formulation is simplified by the parabolic assumption, as outlined by Benedettini et al. [6], while in the latter case discrete formulations and numerical methods are mostly used. Nearly all of the cable discrete models available in the literature were formulated through a space discretization based on the Galerkin approach. This issue is addressed by expanding the displacement functions in the space of the linear eigenfunctions, early obtained in the paper by Irvine and Caughey [8]. By retaining a finite number of degrees of freedom (modal amplitudes), the cable dynamics are thus described by a system of nonlinear ordinary differential equations (ODEs). The approximations contained in such procedures can be anyway in conflict with the complex phenomena under study. A fairly systematic analysis of the influence of the number of modes retained in the discrete model on the accuracy of the predicted nonlinear response was carried out by Arafat and Nayfeh [9]. Among the numerical approaches, many papers focused on the finite element method (FEM) applied to cable modeling in the framework of large displacements (e.g., Desai et al. [10, 11]). A comparison between the analytical Galerkin models and the computational approach based on FEM models, was conducted by Gattulli et al. [12], by adopting the FEM cable representation proposed by Desai [10]. This comparison showed the ability of the FEM procedure to capture most of the coupling and bifurcation phenomena occurring in the cable response. In Ref. [12], it was also underlined that a richer FEM model could even be adopted to verify the basic hypotheses and the suitable dimension of the reduced analytical model. The use of finite element cable models also proved to be

effective in reproducing the experimental behavior of wind-excited suspended cables [13, 14].

In order to study an effective control strategy to reduce the cables vibrations, a particular attention has to be devoted to nonlinear phenomena. In particular, an additional damping in the first out-of-plane mode is of extreme importance in order to prevent out-of-plane bifurcations from occurring. This issue was deeply analyzed in the literature (e.g., [15–22]), albeit many papers limited to the case of planar vibrations control (e.g., [23–27]). A very promising active control solution, able to reduce both in-plane and out-of-plane vibrations, is based on the motion of one cable support. It was proposed by Susumpow and Fujino [16] and was investigated in more recent papers [17–19]. Less expensive solutions are represented by passive and semi-active strategies. Among those, passive dampers mounted transversely to the cable represent probably the most applied solution to dampen in-plane vibrations. References on this topic may be found in [20, 21, 25–27]. The two papers by Xu and Yu [20, 21], in particular, focused on nonplanar vibrations control, while the paper by Abdel–Rohman and Spencer [27] dealt with the mitigation of vertical cable vibrations due to wind-induced galloping. Passive viscous dampers were also applied to many cable stays, although the damper location was typically restricted to the area close to the bridge deck, and this actually reduced the damping effect. A way to increase the control effectiveness, when the damper is close to one anchor, is represented by the use of semiactive dampers. This issue was addressed by Zhou et al. [22] in the case of spatial cable vibrations. Passive tuned mass dampers (TMDs), attached transversely to the cable, were early introduced by Claren and Diana [23]. References to more recent papers on this issue are given in [24, 28–31]. Those devices represent a valid control solution from many points of view. First of all, the position of the devices is not restricted to be close to the anchors. Moreover, their cost is very low if compared to any one of the semiactive or active solutions. On the other side, a single passive TMD device does not exert out-of-plane forces: this does not allow to introduce additional damping in the out-of-plane direction. Besides, the TMD is particularly effective only when the cable vibrates with a well-defined frequency, which usually is the one of the first mode. In order to circumvent these limitations and to enlarge the frequency spectrum of control effectiveness, semiactive TMDs were proposed in the literature [32]. Within this framework, the concept of variable inclination TMD was introduced, in Ref. [33], to reduce the spatial cable vibrations under the action of a turbulent wind.

In this paper, the well-known passive control solution, based on the use of in-plane TMDs, is extended to mitigate the spatial vibrations of shallow cables. This is obtained by adopting a variable out-of-plane inclination TMD attached transversely to the cable at an intermediate point. A simple control algorithm is adopted to regulate the out-of-plane inclination of the TMD. The effectiveness of the proposed control strategy is analyzed by means of numerical simulations, through a FEM formulation and a reduced discrete control-oriented analytical model. Results of both free and harmonically forced vibrations are presented. A detuning analysis toward the first crossover, is also carried out in order to investigate the robustness of the proposed approach against cable slackening.

2 Governing relations

2.1 *Uncontrolled equations of motion*

The nonlinear motion of a suspended cable hanging in the vertical plane Oxy is considered (see Fig. 1). This problem is very well known in the technical literature, since a lot of papers exist that discuss the nonlinear cable dynamics. Therefore, only a brief introduction to such a problem is given here. The cable is modeled as a mono-dimensional linearly elastic continuum with no flexural, torsional or shear rigidities.

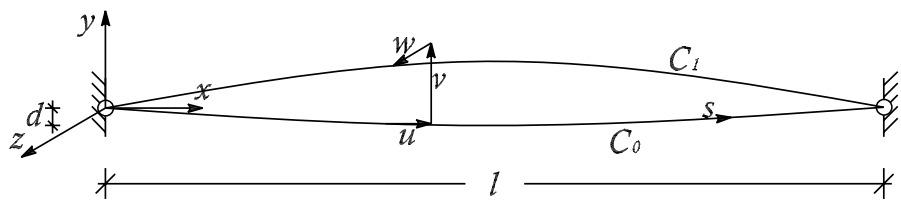

Fig. 1 Cable static and dynamic varied configurations

The supports are placed at the same vertical level and a small sag d to span l ratio is assumed. Under these hypotheses, the infinitesimal curvilinear abscissa element ds can be approximated by dx and the static configuration C_0, described by the function $Y(x)$, assumes the well-known parabolic profile. The displacements $u(x,t)$, $v(x,t)$ and $w(x,t)$, in the coordinate directions, describe the dynamic varied configuration C_1. The equations of motion are thus represented by three partial differential equations in the unknown functions $u(x,t)$, $v(x,t)$ and $w(x,t)$, as early outlined by Benedettini et al. [6]. A further well-known simplification can be made by eliminating the longitudinal component $u(x,t)$, as described in the review paper by Rega [1]. In such a case, a constant strain measure $\bar{e}(t)$ is defined, which is obtained by integrating along the cable the second-order truncation of the elongation. The cable dynamics are thus governed by the following condensed system of two integral-differential equations:

$$\begin{aligned} &\mu\ddot{v} + c_v\dot{v} - \left[Hv' + ES(Y' + v')\bar{e}\right]' = p_y(x,t), \\ &\mu\ddot{w} + c_w\dot{w} - [Hw' + ESw'\bar{e}]' = p_z(x,t) \end{aligned} \tag{1}$$

where E is the Young modulus, S is the cable cross section, H is the horizontal reaction at the two ends, μ, c_v, c_w are the mass and damping coefficients per unit length, and $p_y(x,t)$ and $p_z(x,t)$ are the distributed in-plane and out-of-plane loads, respectively. In (1), a dot and a prime denote derivatives with respect to the time t and to the abscissa x, respectively. The model is completed by homogeneous boundary conditions at $x = 0$ and $x = l$.

2.2 Reduced analytical cable model

At a first stage of investigation, a reduced nonlinear model can be derived from (1) through the standard Galerkin procedure. This is achieved by expanding the cable displacements v and w in the space of the in-plane and out-of-plane modal shapes, respectively. The normalized time $\tau = \frac{t}{\omega_{1v}}$ and abscissa $\chi = \frac{x}{l}$ are introduced, where ω_{1v} is the natural circular frequency of the first in-plane mode, calculated as described in Ref. [8]. The modal coordinates q_i^v and q_k^w, normalized with respect to the cable span l, are introduced to write:

$$\begin{aligned} \frac{v(\chi,\tau)}{l} &= \sum_{i=1}^{\infty} \tilde{v}_i(\chi) q_i^v(\tau), \\ \frac{w(\chi,\tau)}{l} &= \sum_{k=1}^{\infty} \tilde{w}_k(\chi) q_k^w(\tau) \end{aligned} \tag{2}$$

where $\tilde{v}_i$ and $\tilde{w}_k$ are the i-th and k-th in-plane and out-of-plane linear cable eigenfunctions, respectively. A system of nonlinear ordinary differential equations (ODEs) is then written by retaining a certain number of modes (n_v in-plane and n_w out-of-plane modes), by introducing the out-of-plane circular frequencies ω_{iw} and a suitable number of coefficients a_{0ij}, a_{1i} and a_{2ij}:

$$\begin{aligned} &\ddot{q}_i{}^v + \xi_i^v \dot{q}_i{}^v + \sum_{j=1}^{n_v} a_{0ij} q_j^v \\ &\quad + \left(a_{1i} + \sum_{j=1}^{n_v} a_{2ij} q_j^v\right)\bar{e} = p_{iv}, \\ &\ddot{q}_i{}^w + \xi_i^w \dot{q}_i{}^w + \omega_{iw}^2 q_i^w + a_{3i} q_i^w \bar{e} = p_{iw}. \end{aligned} \tag{3}$$

The constant elongation term $\bar{e}$, in (3), is given by:

$$\bar{e} = \sum_{j=1}^{n_v} b_{1j} q_j^v + \sum_{i=1,j=1}^{n_v} b_{2ij} q_i^v q_j^v + \sum_{k=1}^{n_w} b_{3k} q_k^{w\,2} \tag{4}$$

and the in-plane cable circular frequencies can be obtained as $\omega_{iv}^2 = (a_{0ii} + a_{1i} b_{1i})$. The expressions of the coefficients a_{0ij}, a_{1i}, a_{2ij}, a_{3i}, b_{1j}, b_{2ij}, b_{3k} and of the normalized modal loads p_{iv} and p_{iw} can be found in Ref. [12]. As well known in the linear part of system (3), off-diagonal terms $a_{0ij} + a_{1i} b_{1j}$ vanish due to the orthogonality of the eigenfunctions. Nevertheless, modal couplings arise in the nonlinear part, due to quadratic and cubic nonlinearities. Thus, as expected, the modal coordinates introduced in (2) have a different meaning with respect to the modes of linear models. Nevertheless, the modal coordinates are still features of interest in describing the motion and can be employed in a control algorithm to reduce the overall cable vibration.

3 Control strategy

3.1 Suspended cable with variable inclination TMD

The vibration of cables is mainly described by a few modes. The cable motion is, therefore, controllable when additional damping is introduced by a control action in those modes. In linear systems, this would require that the control force has a significant nonzero modal component in all of those modes. In cables, on the contrary, if the first modes (in-plane and out-of-plane) are reduced by the control action, nonlinear coupling terms increase the additional damping of the higher modes. From this point of view, passive TMDs represent a valid control solution, also thanks to their low cost if compared to active solutions.

A transverse TMD is applied here to reduce the in-plane cable vibrations (see Fig. 2a). The device is tuned on the frequency of the first mode and the damping coefficient is set to the optimum value. The position of the device is selected at $x_0 = l/4$, where both the first symmetric and the first anti-symmetric modes have a nonzero modal component. The control device is designed to have a variable inclination ε in the Oyz plane (see Fig. 2b). In this way, the TMD exerts on the cable a force that has, in general, an in-plane component ξ and an out-of-plane one ζ. The inclination ε is then regulated by a semiactive strategy, as explained in the following. The axis r of the TMD is adopted as the local reference system (see Fig. 2b). The angle between r and the vertical axis y in the Oxy plane is denoted by α. The relative displacement V between the mass m and the cable node is aligned with r. As shown in Fig. 2b, it is positive when the mass and the cable node approach each to the other. The initial distance ($V = 0$) between the mass and the cable is denoted by R. Thus $R - V$ is the distance at the general configuration ($V \neq 0$).

3.2 Controlled equations of motion

Under the hypothesis of small-sagged cable, it is possible to assume $\cos(\alpha) \cong 1$ and $\sin(\alpha) \cong 0$. Consequently, the horizontal in-plane component of the con-

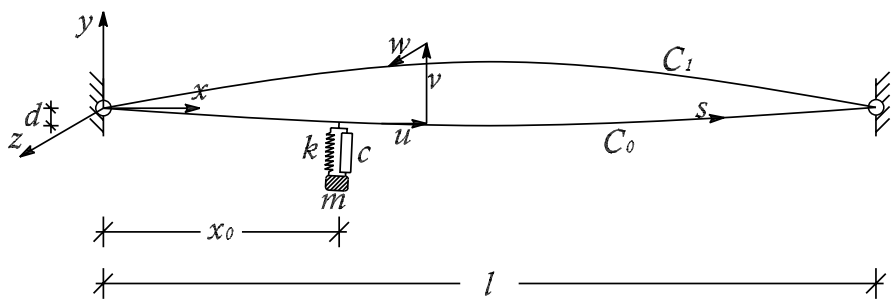

(a)

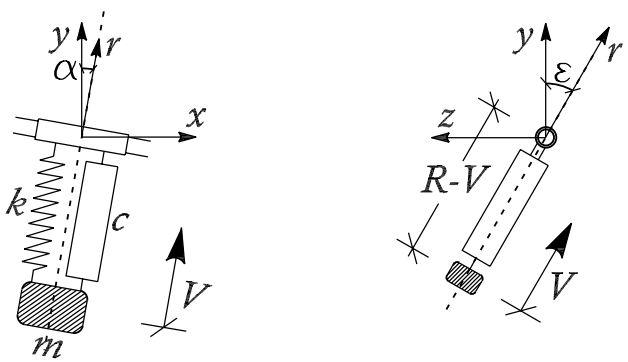

(b)

Fig. 2 Cable equipped with a semiactive TMD (**a**); plane projections of the TMD device with local reference system (**b**)

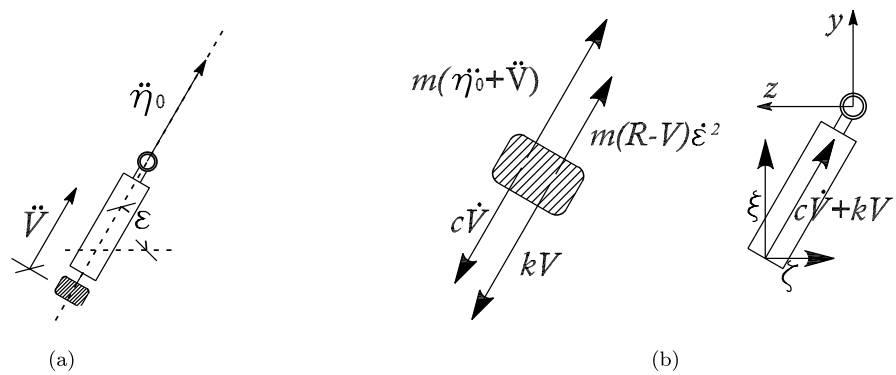

Fig. 3 Accelerations of the TMD (**a**); control forces (**b**)

trol force is negligible, while the (vertical) in-plane and out-of-plane control forces read as:

$$\begin{aligned}\xi(t) &= [kV + c\dot{V}]\cos(\varepsilon),\\ \zeta(t) &= [kV + c\dot{V}]\sin(\varepsilon).\end{aligned} \tag{5}$$

The forces ξ and ζ can thus be introduced in the condensed model, by means of the Dirac δ-function $\delta(x - x_0)$, leading to the following equations of motion:

$$\begin{aligned}&\mu\ddot{v} + c_v\dot{v} - \left[Hv' + ES(Y' + v')\bar{e}\right]'\\ &\quad = p_y(x,t) + \xi(t)\delta(x - x_0),\\ &\mu\ddot{w} + c_w\dot{w} - [Hw' + ESw'\bar{e}]'\\ &\quad = p_w(x,t) + \zeta(t)\delta(x - x_0)\end{aligned} \tag{6}$$

with homogeneous boundary conditions at $x = 0$ and $x = l$. As mentioned previously, $x_0 = l/4$ is the TMD position.

The main effect of the TMD is to exert a force along the r direction. The motion of m along such a direction is represented in Fig. 3a, where the local acceleration $\ddot{V}$ is summed with the transport acceleration $\ddot{\eta}_0$ of the node at $x = x_0$, projected along the r direction. The motion of m is then described by the following equation (see Fig. 3b):

$$m\left(\ddot{V} + \ddot{\eta}_0 + (R - V)\dot{\varepsilon}^2\right) = -c\dot{V} - kV \tag{7}$$

where the right-hand side represents the total control force along r. Equation (7) is written under the only hypothesis that the weight of the small mass is negligible with respect to the other forces involved, as usually assumed in the literature concerning TMD dampers on cables (see, for example, [24, 29–31] among others). As expected, this assumption is valid for very small m and rather taut cables. It is verified in Sect. 4.2 for the case study. The term $V\dot{\varepsilon}^2$ in (7) may also be neglected, as a higher order term with respect to $R\dot{\varepsilon}^2$. This hypothesis is assumed in the following developments and verified in Sect. 4.2.

3.3 Reduced analytical and FEM models of the controlled cable

The presence of the control force produces a change in the natural frequencies and in the modal shapes $\tilde{v}_i$ and $\tilde{w}_i$ calculated by Irvine's theory [8]. The problem is analyzed in the Appendix, where the free in-plane vibrations of a general cable with a passive TMD, anchored at $x = x_0$, are considered. As shown there, the modification introduced in the system is small when the ratio $\gamma = \frac{m}{\mu l}$ between the mass of the TMD and the mass of the overall cable tends to zero. Nevertheless, a significant change in the modal shape and modal frequency of the first mode (to which the TMD is tuned) should be expected, even with small γ, as x_0 approaches the value $l/2$.

3.3.1 Reduced analytical model

The modification introduced by the TMD in the system must be taken into account in the reduced Galerkin model, in order to get a high numerical accuracy. To this end, the modal shapes and the natural frequencies, modified by the presence of the TMD, are considered to expand v and w. A control-oriented analytical model is thus obtained, in which four in-plane and four out-of-plane modes are retained. The control forces are introduced in the system by means of their

modal components:

$$\begin{aligned}
&\ddot{q}_i^{\,v} + \xi_i^v \dot{q}_i^{\,v} + \sum_{j=1}^{n_v} a_{0ij} q_j^v + \left(a_{1i} + \sum_{j=1}^{n_v} a_{2ij} q_j^v \right) \bar{e} \\
&\quad = p_{iv} + c_i^v \xi(\tau), \\
&\ddot{q}_i^{\,w} + \xi_i^w \dot{q}_i^{\,w} + \omega_{iw}^2 q_i^w + a_{3i} q_i^w \bar{e} = p_{iw} + c_i^w \zeta(\tau)
\end{aligned} \tag{8}$$

where the coefficients c_i^v and c_i^w are calculated as:

$$\begin{aligned}
c_i^v &= \frac{1}{\mu l \omega_{1v}^2} \frac{\int_0^1 \delta(\chi - \chi_0)\phi_i(\chi)\, d\chi}{\int_0^1 \phi_1^2(\chi)\, d(\chi)} \\
&= \frac{1}{\mu l \omega_{1v}^2} \frac{\phi_i(\chi_0)}{\int_0^1 \phi_1^2(\chi)\, d\chi}, \\
c_i^w &= \frac{1}{\mu l \omega_{1v}^2} \frac{\int_0^1 \delta(\chi - \chi_0)\psi_i(\chi)\, d\chi}{\int_0^1 \phi_1^2(\chi)\, d\chi} \\
&= \frac{1}{\mu l \omega_{1v}^2} \frac{\psi_i(\chi_0)}{\int_0^1 \phi_1^2(\chi)\, d\chi}
\end{aligned} \tag{9}$$

and $\chi_0 = x_0/l$. The analytical model described by (8) is utilized in Sects. 4.4 and 4.5 to investigate the damping effect of the proposed control strategy under forced harmonic vibrations and to analyze detuning effects.

3.3.2 FEM model

As discussed in Sect. 2.2, reduced Galerkin models apply to shallow cables for which the condensation hypothesis can be made. A way to circumvent such a limitation is represented by the FEM method, which applies to arbitrarily sagged cables, even when subjected to horizontal external forces. Within this paper, the FEM approach described by Cluni et al. [13] is adopted and the cable is described by a finite number n of three-dimensional nonlinear trusses. By denoting with $\mathbf{U} = (u_1, v_1, w_1, \ldots, u_n, v_n, w_n)^T \in \mathbb{R}^{3(n+1)}$ the vector of nodal displacements, the well-known equations of motion are derived following the classical *updated Lagrangian* approach, in the framework of large displacements and small strains. A Rayleigh damping matrix is assumed in those equations, with mass coefficient α_C and stiffness coefficient β_C. The time integration of the system of ODEs is carried out through the Hilber–Hughes–Taylor algorithm [36] and the numerical solution at the generic time $t + \Delta t$ is calculated through the Newton–Raphson scheme, with a linear initial estimate of the vector of restoring forces. The vector of displacement increments $\mathbf{\Delta U}(t + \Delta t)$ is thus calculated iteratively until the error σ^k at the k-th iteration satisfies:

$$\sigma^k = \sqrt{\left| \frac{\delta \mathbf{U}^{k^T} \delta \mathbf{U}^k}{\mathbf{U}^{k^T} \mathbf{U}^k} \right|} < \tilde{\sigma} \tag{10}$$

where $\mathbf{\Delta U}(t + \Delta t) = \sum_{i=1}^{k} \delta \mathbf{U}^i$ and $\tilde{\sigma}$ is a given tolerance. The above described method is second order accurate and the conditions for its stability are given in Ref. [36].

Two finite element models are implemented within this paper, following the steps described above. The former is written in the Ansys CivilFem environment [34] (ACF model) and considers the only in-plane TMD ($\varepsilon(t) = 0$), reproduced through a specific visco-elastic element without neglecting the weight of the mass m. Since the variable inclination TMD can hardly be implemented in a commercial environment, a FEM model of controlled cable is also written in the MatLab environment [35] (MTL model), with no restrictions on the device inclination ε. In such a model, the motion of the small mass m is calculated through a second order finite difference discretization of (7), under the hypothesis of neglecting the term $V\dot{\varepsilon}^2$:

$$\begin{aligned}
&V(t + \Delta t) \\
&\quad = \left(1 + \frac{c\Delta t}{2m} + \frac{k\Delta t^2}{m}\right)^{-1} \left(2V(t) + \left(\frac{c\Delta t}{2m} - 1\right)\right. \\
&\qquad \times V(t - \Delta t) \\
&\qquad \left. - \Delta t^2 \left(\ddot{\eta}_0 + R\left(\frac{\varepsilon(t + \Delta t) - \varepsilon(t - \Delta t)}{2\Delta t}\right)^2\right)\right).
\end{aligned} \tag{11}$$

As already observed in the case of (7), (11) is written under the assumption that the weight of the small mass m is negligible with respect to the other forces involved. Such an assumption is verified in Sect. 4.2 for the case study, by means of a comparison with the ACF model. The inclination $\varepsilon(t + \Delta t)$ is calculated, at any time step, according to the feedback control law introduced in Sect. 3.4 and the control forces are calculated as described by (5). It is worth noting that all the three components of the control forces are considered either in the ACF or in the MTL models, since the hypothesis of small angle α is not required in the FEM formulation.

A total number $n = 11$ of unconstrained nodes is considered to discretize the cable, leading to a 33 de-

grees of freedom system. The initial static configuration C_0 (reference condition) is achieved by assigning the self-weight to the nodes in a quasi-static way, starting from a parabolic shape. The ACF and MTL models give almost similar results, as briefly discussed in Sect. 4.2. The former is adopted in order to compare the (numerical) natural frequencies of the cable-TMD system with those analytically obtained in Appendix. The latter approach (MTL) is then utilized, in Sect. 4.3, in order to show the damping properties of the proposed control strategy under free spatial vibrations.

3.4 Control law

A inner in-plane TMD is considered herein in order to investigate its behavior when the out-of-plane inclination is regulated. In-plane control of cable vibrations, utilizing passive TMDs, has been deeply investigated in the literature and its effectiveness is shown in Refs. [21, 24, 28–31]. The small degradation of the in-plane control performance, due to the out-of-plane inclination, is pointed out in Sect. 4 and justifies the use of the linear TMD. A mass ratio $\gamma < 2\%$ is assumed, in order to have a small modification of the dynamic properties of the system. The effectiveness of the TMD is, therefore, maximum for the first mode and decreases as the modal order increases. Nevertheless, a damping increment is expected even in higher modes.

As already specified, the variable inclination ε is employed to control the out-of-plane vibrations, by means of the control force $\zeta(t) = [kV(\varepsilon) + c\dot{V}(\varepsilon)] \times \sin(\varepsilon)$. The dependence of V and its derivatives on ε is expressed by (7). The following linear velocity feedback is here considered in order to regulate ε:

$$\varepsilon = g_{\varepsilon 1} \cdot \dot{\bar{q}}_1^w + g_{\varepsilon 2} \cdot \dot{\bar{q}}_2^w \tag{12}$$

where $g_{\varepsilon 1}$ and $g_{\varepsilon 2}$ are user-defined control gains and $\bar{q}_1^w$ and $\bar{q}_2^w$ represent two estimates of the first and the second out-of-plane modal amplitudes, as defined in the following. The interval $0 < \varepsilon(t) < \pi$ has to be considered to limit the values of ε. By substituting (7) into the expression of ζ one obtains:

$$\zeta(t) = -m\big(\ddot{V}(\varepsilon, t) + \ddot{\eta}_0(\varepsilon, t) + (R - V)\dot{\varepsilon}^2\big)\sin(\varepsilon). \tag{13}$$

In order to justify the damping capability of (13), let us consider its expression for small ε, by adopting the approximation $\sin\varepsilon \cong \varepsilon$ and by assuming that the first order approximations of $\ddot{V}$ and $\ddot{\eta}_0$ do not depend on ε:

$$\zeta \cong -m\big(\ddot{V} + \ddot{\eta}_0 + (R - V)\dot{\varepsilon}^2\big)\varepsilon + O\big(\varepsilon^3\big). \tag{14}$$

Putting (12) into (14), one obtains:

$$\begin{aligned}\zeta \cong -m\big(\ddot{V} + \ddot{\eta}_0 + (R - V)\big(g_{\varepsilon 1} \cdot \ddot{\bar{q}}_1^w + g_{\varepsilon 2} \cdot \ddot{\bar{q}}_2^w\big)^2\big) \\ \times \big(g_{\varepsilon 1} \cdot \dot{\bar{q}}_1^w + g_{\varepsilon 2} \cdot \dot{\bar{q}}_2^w\big).\end{aligned} \tag{15}$$

Equation (15) represents the feedback out-of-plane control force, evaluated for small ε. It contains the derivative terms $\dot{\bar{q}}_1^w$ and $\dot{\bar{q}}_2^w$, which can have a well-known damping effect [16, 17]. Nevertheless, even when ε is small, (15) is nonlinear due to the presence of quadratic terms in the modal accelerations. Moreover, when ε is large, nonlinearity of the control action is enhanced by the dependence of $\ddot{V}$ and $\ddot{\eta}_0$ on ε and the approximation $\sin(\varepsilon) \cong \varepsilon$ becomes inadequate. These considerations allow to classify ζ as generated by a nonlinear velocity feedback. Within this framework, polynomial control laws were applied and discussed in Ref. [19], where the effectiveness of a nonlinear velocity feedback is shown for out-of-plane cable vibrations mitigation, through longitudinal control.

Within the semiactive strategy described by (12), two monitored points are here considered. A proper positioning of such nodes is required so as to have the first two out-of-plane modes observable. The monitored points are placed at $x = l/4$ and $x = 3l/4$ and the corresponding out-of-plane displacements w_{1q} and w_{3q} are observed. Their expression in terms of normalized modal amplitudes is given by (2). By truncating this expression at the second order out-of-plane mode, one obtains:

$$\begin{aligned}w_{1q} &\cong l \cdot \big(\tilde{w}_1(1/4)\bar{q}_1^w + \tilde{w}_2(1/4)\bar{q}_2^w\big), \\ w_{3q} &\cong l \cdot \big(\tilde{w}_1(3/4)\bar{q}_1^w + \tilde{w}_2(3/4)\bar{q}_2^w\big).\end{aligned} \tag{16}$$

In the uncontrolled case, the following relations hold true between the out-of-plane mode shapes: $\tilde{w}_1(1/4) = \tilde{w}_1(3/4)$ and $\tilde{w}_2(1/4) = -\tilde{w}_2(3/4)$. Since the control device produces no modifications on $\tilde{w}_1$ and $\tilde{w}_2$, those assumptions are true also in the controlled case. The estimates $\bar{q}_1^w$ and $\bar{q}_2^w$ can thus be obtained by sum-

mation and subtraction of the two equations (16), as outlined in Ref. [18]:

$$\bar{q}_1^w \cong \frac{w_{1q} + w_{3q}}{l \cdot (\tilde{w}_1(1/4) + \tilde{w}_1(3/4))},$$
$$\bar{q}_2^w \cong \frac{w_{1q} - w_{3q}}{l \cdot (\tilde{w}_2(1/4) - \tilde{w}_2(3/4))}. \quad (17)$$

4 Numerical example

4.1 The case study

The results described in Sects. 4.2, 4.3, 4.4 and 4.5 are referred to a sample cable $\mathfrak{C}^1$ with the nondimensional parameters: $\psi = EA/H = 10970$ and $\nu = d/l = 0.0064$. These values of the parameters ψ and ν correspond to a value of the stiffness nondimensional Irvine parameter $\lambda^2 = 2.76\pi^2$. Since $\lambda^2 < 4\pi^2$, the cable $\mathfrak{C}^1$ is on the left of the first crossover point. This means that the first in-plane symmetric mode has a frequency f_1^v that is lower than the frequency of the first antisymmetric mode f_2^v and that the cable remains in tension for any amplitude of vibration. A mass ratio $\gamma = 0.018$ is assumed to design the TMD device, which is tuned on the first in-plane cable frequency.

The presence of the passive in-plane TMD produces a small change in the first two in-plane modal shapes, as described in the Appendix, while higher order eigenfunctions are practically identical either with or without the passive TMD. The difference between the first two in-plane controlled and uncontrolled eigenfunctions, normalized to the absolute maximum value, is shown in Figs. 4a and b. The Rayleigh damping matrix of the cable $\mathfrak{C}^1$ is calculated with the values $\alpha_C = 0.027$ and $\beta_C = 0.0004$, which correspond to the modal damping ratios ξ_i summarized in Table 1. In the following developments, the results refer to v_m and w_m, which are the mid-span vertical and out-of-plane cable displacements, respectively.

4.2 Models validation

In order to verify the correspondence of the adopted models, the results of some preliminary checks are reported for the uncontrolled and controlled cases. A comparison between the analytic and numeric natural frequencies of the cable is first performed to evaluate the adequateness of the mesh refinement of the FEM models. Afterwards, the assumptions made in Sect. 3.2 are validated to some extent.

The first 8 natural frequencies of the cable $\mathfrak{C}^1$ are obtained numerically, by eigenvalue analysis, in both MTL and ACF models, at the static configuration C_0. Those values are compared to the analytical ones, calculated by Irvine's theory [8], in Table 1. The first

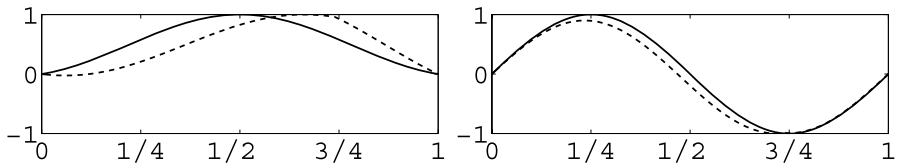

(a) First in-plane mode (b) Second in-plane mode

Fig. 4 Uncontrolled (*solid line*) vs. controlled (*dashed line*) eigenfunctions of the cable $\mathfrak{C}_1$

Table 1 Natural frequencies of the cable $\mathfrak{C}^1$ with and without the passive in-plane TMD: f_i^v and f_i^w denote the i-th in-plane and out-of-plane natural frequencies, respectively

Mode	ξ_i	Without TMD			With TMD	
		Analytical	MTL	ACF	Analytical	ACF
f_1^v	0.0110	3.910	3.945	3.932	3.679	3.600
f_2^v	0.0122	4.416	4.464	4.446	4.560	4.694
f_3^v	0.0180	6.747	6.916	6.884	6.739	6.982
f_4^v	0.0237	8.832	9.232	9.197	8.832	9.263
f_1^w	0.0075	2.208	2.213	2.204	2.208	2.220
f_2^w	0.0122	4.416	4.463	4.446	4.416	4.478
f_3^w	0.0177	6.624	6.791	6.765	6.624	6.813
f_4^w	0.0237	8.832	9.232	9.198	8.832	9.263

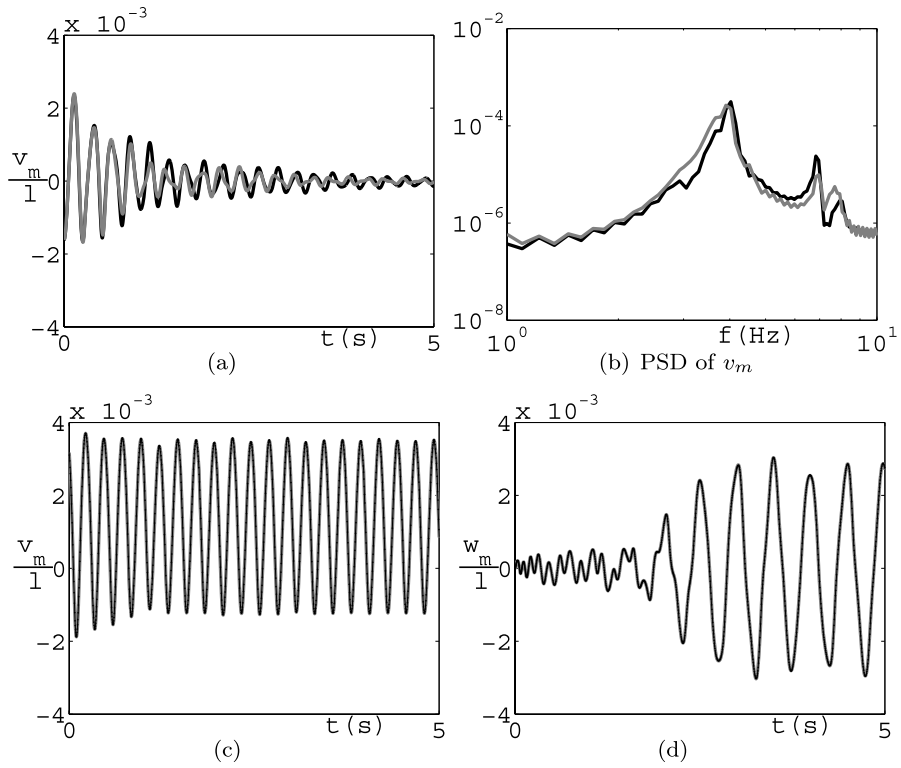

Fig. 5 In-plane controlled free vibrations with MTL (*black line*) and ACF (*grey line*) models: time domain comparison (**a**), frequency domain comparison (**b**); comparison of in-plane and out-of-plane mid-span displacements under forced harmonic in-plane vibrations, by neglecting (*grey line*) or retaining (*black dots*) the term $V\dot{\varepsilon}^2$ in (7): (**c**), (**d**)

8 natural frequencies of the cable with the passive in-plane TMD are also calculated in the ACF model. The obtained values are compared to those analytically given in the Appendix. A small change in the first two in-plane natural frequencies is caused by the presence of the TMD. Higher frequencies are practically identical between the uncontrolled and controlled cases. The good agreement between numeric and analytical values, indicates that the adopted number of elements is sufficient to describe the dynamics of the cable with high accuracy.

The hypothesis of neglecting the weight of the mass m in (7) has proved to be valid for the case under study. As previously observed, such a weight is neglected in the MTL model, while it is retained in the ACF model. Nevertheless, the two approaches give practically identical results, as shown, for instance, in Figs. 5a and b, for a sample case of free in-plane oscillations. Both time domain and frequency domain comparisons are reported in such a figure to confirm the equivalence of the two models. The power spectral density (PSD) function of v_m is considered in the frequency domain comparison. The term $V\dot{\varepsilon}^2$, that appears in (7) has also proved to be negligible for the studied case. As an example, the relevance of such a term is analyzed in Figs. 5c and d for a special case of forced harmonic vibrations, in resonance with the first in-plane mode. The forcing load has the shape of the first in-plane mode and modal amplitude $p_{1v} = 0.001$. As better discussed in Sect. 4.4, a bifurcated spatial motion occurs in the considered case, and thus the centrifugal term in (7) plays a fundamental role in the system dynamics. From Figs. 5c and d, one sees that neglecting the term $V\dot{\varepsilon}$ in (7) does not produce significant differences in the results. Thus, in the following investigations, such a term is neglected. In order to verify the suitable dimension of the reduced model, the results of the FEM models and of the Galerkin ones were also compared. The use of four in-plane and four out-of-plane modes has proved to be sufficient to describe the cable dynamics with a good approximation. As an example, the results of two free uncontrolled vibrations are compared in Figs. 6a and b.

4.3 Controlled free vibrations

The free nonplanar vibrations of the cable $\mathfrak{C}_1$ are considered here in the controlled and uncontrolled cases. The simulations are performed through the MTL FEM

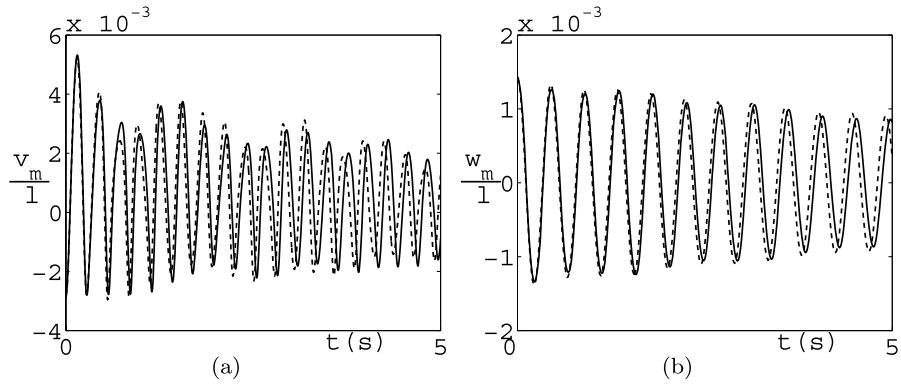

Fig. 6 Mid-span uncontrolled free in-plane and out-of-plane vibrations with MTL (*solid line*) and Galerkin (*dashed line*) models: (**a**), (**b**)

Table 2 Analysis cases for nonlinear free vibrations

Case	$q_1^v(0) \times 10^{-3}$	$q_2^v(0) \times 10^{-3}$	$q_1^w(0) \times 10^{-3}$
A	2.8	−0.4	0.0
B	4.8	−0.7	0.0
C	0.0	0.0	−2.4
D	2.7	−0.4	−1.4

model described in Sect. 3.3.2. Four different cases of free vibrations are considered, with the modal initial conditions reported in Table 2. In-plane initial conditions are considered in cases *A* and *B*. In particular, these initial conditions are such that a planar motion occurs in case *A*, while a bifurcated out-of-plane motion occurs in case *B*. Case *C* considers the free vibrations of the first out-of-plane mode, with a small participation of the other modes. Finally, in case *D*, initial conditions are given to both in-plane and out-of-plane modes, leading to a free spatial motion. It is worth noting that in all the considered cases, the amplitudes of vibrations are large enough that nonlinear phenomena govern the motion.

Figure 7 shows the most significant controlled and uncontrolled mid-span displacements in the cases reassumed in Table 2. The vertical and out-of-plane displacements, v_m and w_m, are normalized with respect to the cable span l. The results show that the control strategy introduces a significant additional damping in both in-plane and out-of-plane modes. The out-of-plane control effectiveness is of particular interest. First of all, bifurcated out-of-plane oscillations, in case *B*, are significantly reduced by the control strategy. Moreover, case *D* shows that the variable inclination TMD is able to control a spatial motion, occurring starting from in-plane and out-of-plane nonzero initial conditions. Out-of-plane bifurcation is not observed in case *A*, while in case *C* out-of-plane displacements prevail on the in-plane ones. The angle $\varepsilon(t)$ in case *C*, regulated by (12), is also represented in Fig. 8.

4.4 Harmonic analysis

The control-oriented Galerkin model described in Sect. 3.3.1 is here adopted in order to analyze the effectiveness of the semiactive TMD under harmonic in-plane excitation. The cable is subjected to a sinusoidal load, with the shape of the first in-plane mode and a modal amplitude $p_{1v} = 0.001$. The circular frequency Ω of such a load, normalized to the natural circular frequency of the first in-plane mode w_{1v}, is varied around the primary resonance. It is worth noting that the value of w_{1v}, to which Ω is normalized, changes in the controlled and uncontrolled cases. Four in-plane and four out-of-plane modes are considered in the model. The modal shapes and natural frequencies of the system composed by the cable and the passive TMD are considered to derive the model in the controlled case, as described in the Appendix.

The results of the harmonic analysis are represented in Figs. 9a and b, by means of uncontrolled and controlled frequency response curves q_1^v vs. Ω and q_1^w vs. Ω. In order to detect softening and hardening branches, as well as dynamic equilibrium bifurcation points, the periodic solutions are evaluated, in the MatLab environment through a sequential continuation with sweeping variation of the frequency. This means that once the solution $(q_1^v, q_1^w, \ldots, q_4^v, q_4^w, \dot{q}_1^v, \dot{q}_1^w, \ldots, \dot{q}_4^v, \dot{q}_4^w)$ at a given frequency Ω is known, the response at an increased frequency $\Omega + \Delta\Omega$ is evaluated by integrating the equations of motion in time with initial conditions

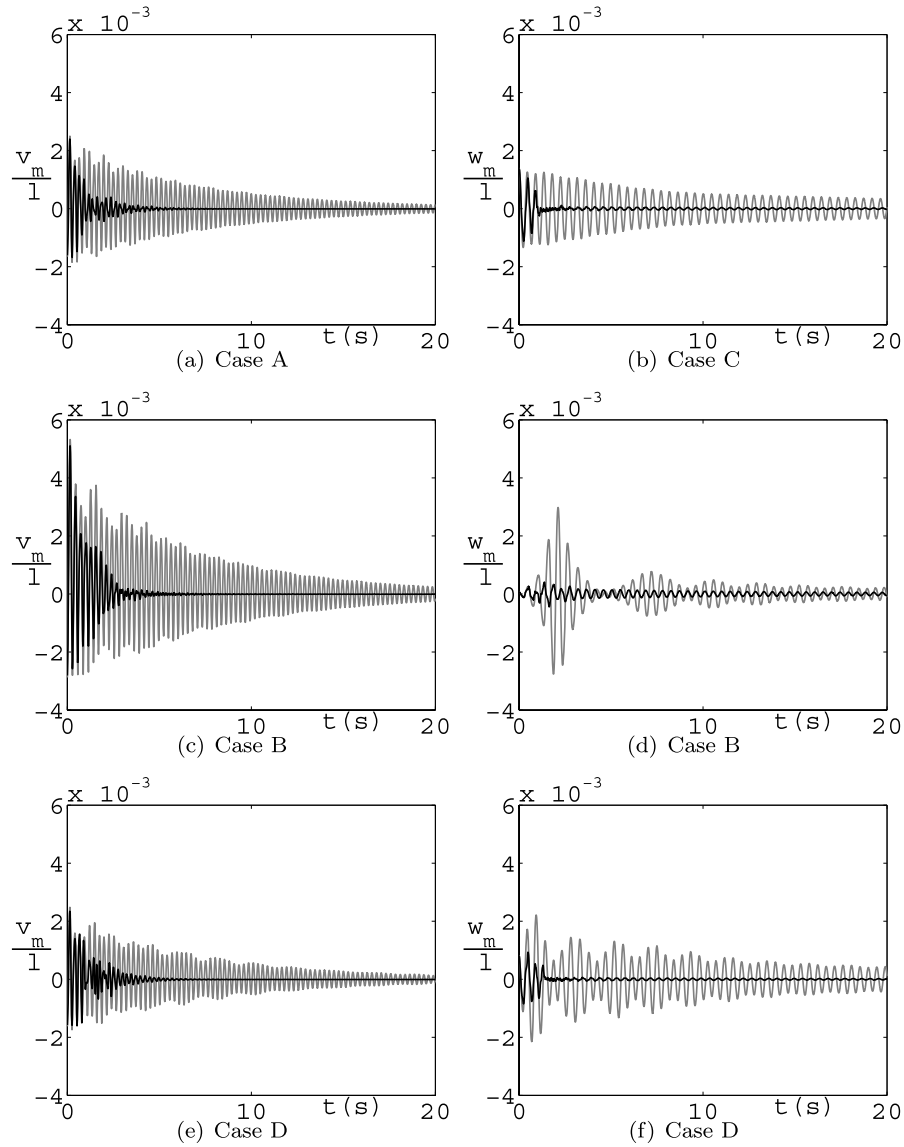

Fig. 7 Nonlinear free vibrations (uncontrolled in *grey*, controlled in *black*)

$(q_1^v, q_1^w, \ldots, q_4^v, q_4^w, \dot{q}_1^v, \dot{q}_1^w, \ldots, \dot{q}_4^v, \dot{q}_4^w)$. A Runge–Kutta method of order 4, with a global error tolerance of 10^{-6}, is assumed for the time integration of the system of ODEs, since it revealed to be a good compromise between computational efficiency and numerical accuracy (the global error is governed by the step size to the power of 5). A suitable predictor-corrector method is coded to modify the initial conditions until they coincide with the periodic amplitudes. Only stable solutions can be detected with such an approach. The results show that the control strategy highly reduces the in-plane modal amplitudes q_1^v in the region of the primary resonance. A strong $1:2$ ($\Omega = 0.5$) resonant peak is also observed in the uncontrolled case that is completely damped out by the control action. The modal amplitude p_{1v} is selected in such a way that a strong out-of-plane bifurcation occurs in the uncontrolled case, in all the considered frequency domain. As it can be observed, the control action is able to highly control such a motion. Moreover, the bifurcation appears with small amplitudes, only in the region which can roughly be identified with the interval $0.4 < \Omega < 1.1$. Figures 9c and d show the behavior of the antisymmetric in-plane and out-of-plane modes. These figures show that the stable harmonic modal amplitudes q_2^v and q_2^w are significantly smaller than

q_1^v and q_1^w. Nevertheless, the participation of the antisymmetric modes is a little enhanced by the control action, in both in-plane and out-of-plane vibrations. This is due to the introduction of the modal components $c_2^v\xi(t)$ and $c_2^w\zeta(t)$ in (8). In the out-of-plane motion, in particular, the antisymmetric mode q_2^w is kept small by the second term of (12). Without such a term, instability of q_2^w would easily arise. The bifurcation of the third in-plane mode is observed in Fig. 9e, in the uncontrolled case, around the primary resonance. The participation of q_3^v is practically damped out by the control action, thus confirming the capability of the TMD to introduce additional damping even in higher modes.

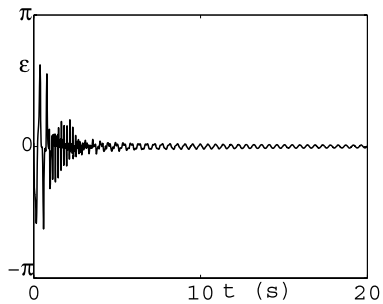

Fig. 8 Variable inclination $\varepsilon(t)$ in case *C*

Four state-space projections of the stable periodic orbits, evaluated at $\Omega = 0.4$ and $\Omega = 1.0$, are represented in Fig. 10. The control strategy significantly reduces the amplitudes of the stable limit cycles. In the case $\Omega = 0.4$, the vicinity of the $1:2$ resonance is clearly evident in the uncontrolled case. The same resonance is not visible in the controlled case. Out-of-plane bifurcation is prevented by the control action for $\Omega = 0.4$. At $\Omega = 1.0$, such a bifurcation appears also in the controlled case but with considerably lower amplitudes with respect to the uncontrolled solution.

4.5 Detuning analysis

Steel cables are subjected, in structural applications, to slackening, which causes the progressive increment

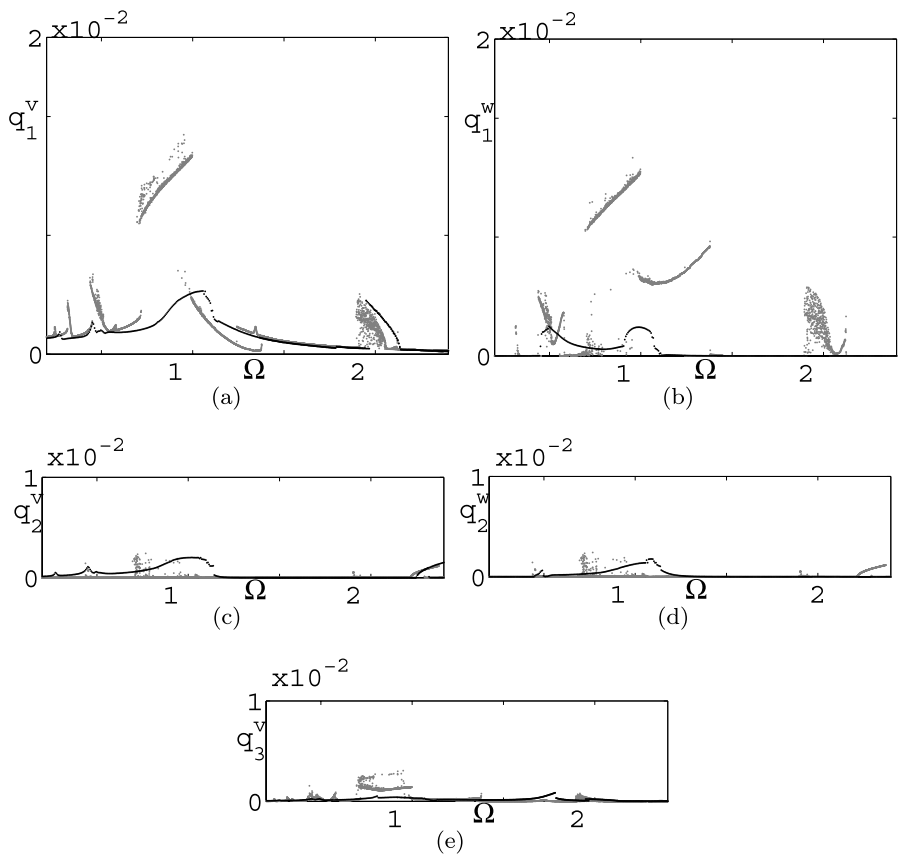

Fig. 9 Harmonic analysis with sequential continuation: the *dots* represent the stable solutions (uncontrolled in *grey*, controlled in *black*)

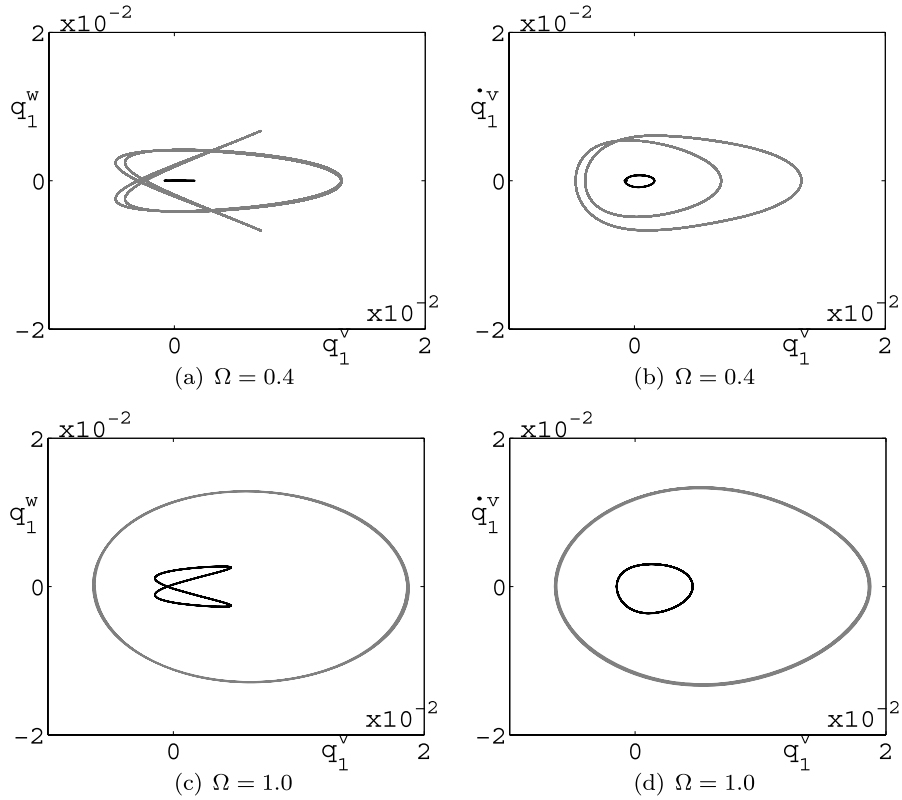

Fig. 10 Phase plane projections of significant harmonic solutions (uncontrolled in *grey*, controlled in *black*)

of the sag, with consequent growth of the Irvine parameter λ^2. This aspect is significant in control applications for two fundamental reasons. The former reason is that a variation of λ^2 determines a modification of the natural frequencies and mode shapes of the cable. When the cable is placed on the left of the first crossover point, this leads to a migration toward the internal resonance between the first two in-plane modes and the second out-of-plane mode. It is well known (see, for example, [1–6] among others) that internal resonance conditions produce a richness of modal instabilities that could reduce the effectiveness of the control strategy. The latter reason is that the in-plane TMD is usually tuned on the frequency of the first in-plane mode. A change in such a frequency produces, therefore, a detuning of the device, which reduces its damping capability.

In order to investigate the robustness of the proposed control strategy to slight variations of the Irvine parameter and consequent detuning of the control device, the slackening of the cable $\mathfrak{C}_1$ is considered herein. An increment of 5%, 10% and 12% of the sag d makes λ^2 assume the values $3.20\pi^2$, $3.68\pi^2$ and $3.89\pi^2$, respectively. The ratios between the circular frequencies of the second in-plane and out-of-plane modes and the circular frequency of the first in-plane mode (ω_{2v}/ω_{1v} and ω_{2w}/ω_{1v}) are reported in Table 3 for the considered values of the Irvine parameter. Such a table shows that the cable $\mathfrak{C}_1$, in the uncontrolled case ($\lambda^2 = 2.76\pi^2$), is not far from the internal resonances occurring at the first crossover ($\omega_{2v}/\omega_{1v} = 1$, $\omega_{2w}/\omega_{1v} = 1$). The presence of the TMD causes an increment of the ratio ω_{2v}/ω_{1v} and slightly withdraws the cable from those resonances. The considered cases of slackening are such that, as the sag is increased, the ratios ω_{2v}/ω_{1v} and ω_{2w}/ω_{1v} migrate towards the

Table 3 Cases of detuning analysis

λ^2/π^2	Without TMD		With TMD	
	ω_{2v}/ω_{1v}	ω_{2w}/ω_{1v}	ω_{2v}/ω_{1v}	ω_{2w}/ω_{1v}
2.76	1.129	1.129	1.239	1.129
3.20	1.077	1.077	1.194	1.153
3.68	1.028	1.028	1.141	1.103
3.89	1.009	1.009	1.063	1.034

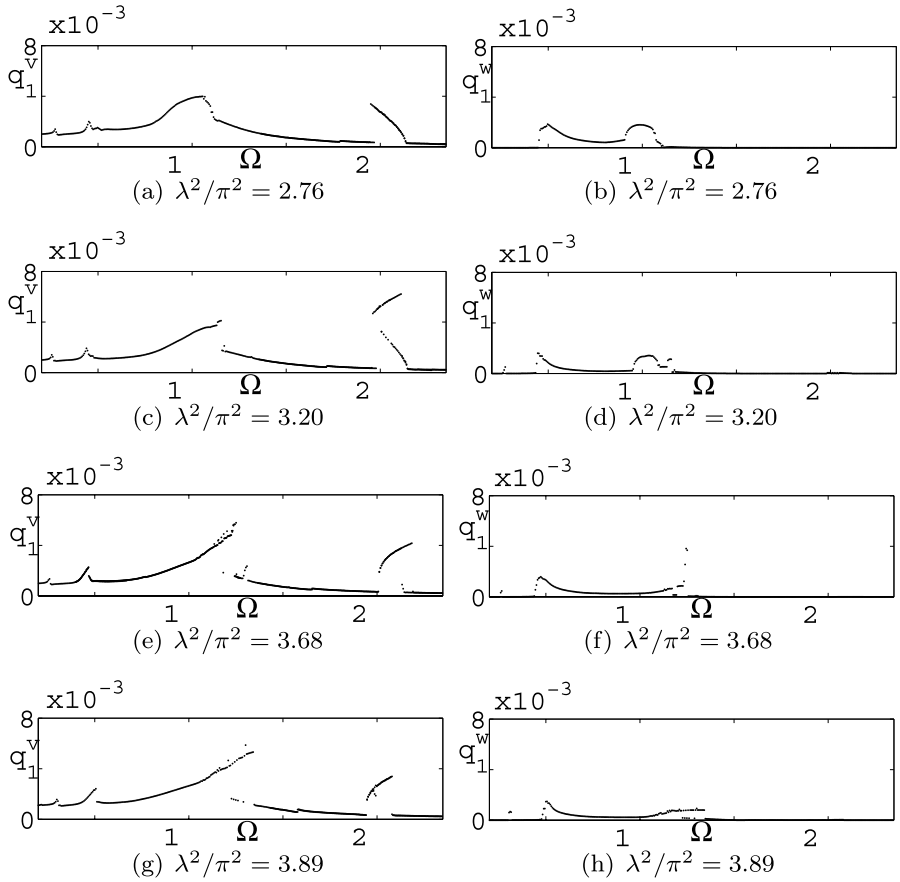

Fig. 11 Controlled frequency response curves by varying the Irvine parameter of the cable

value 1 and thus the cable $\mathfrak{C}_1$ is brought closer to the internal resonance conditions occurring at the first crossover.

The controlled frequency response curves q_1^v vs. Ω and q_1^w vs. Ω, evaluated in the cases reported in Table 3, are represented in Fig. 11. Figures 11a and b, in particular, represent the stable harmonic solutions without detuning, while Figs. 11c, d, e, f, g and h report the solutions with detuning. From those figures, the robustness of the out-of-plane control strategy, with respect to variations of λ^2, is clearly pointed out. The frequency response curves q_1^w vs. Ω remain, in fact, substantially equivalent as λ^2 increases. In-plane control, as expected, is a little more sensitive to detuning effects. Even if the peak values do not sensibly increase when detuning occurs, a 5% increment of sag ($\lambda^2 = 3.20\pi^2$) produces a clear hardening behavior of q_1^v around the primary resonance, which causes well-known jump phenomena. This behavior is even more evident when 10% and 12% increments of sag are considered ($\lambda^2 = 3.68\pi^2$ and $\lambda^2 = 3.89\pi^2$). Besides, the 2 : 1 resonant peak ($\Omega = 2.0$), that is represented by a softening stable branch with no detuning, assumes a softening-hardening aspect for $\lambda^2 = 3.20\pi^2$ and becomes completely hardening for $\lambda^2 = 3.68\pi^2$ and $\lambda^2 = 3.89\pi^2$. This, in particular, produces a strong resonant peak, in the case $\lambda^2 = 3.20\pi^2$, which is even larger than the 1 : 1 peak ($\Omega = 1.0$) and represents a region of poor control performance.

5 Conclusions and future developments

In this paper, the well-known passive control solution, based on the use of tuned mass dampers to reduce the in-plane vibrations of cables, is extended to mitigate also the out-of-plane oscillations. This is achieved by adopting a variable out-of-plane inclination TMD attached transversely to the cable at an intermediate point. A linear velocity feedback, based on the observation of two points, is designed aiming at regulating the out-of-plane inclination of the TMD.

A geometric nonlinear finite element model of controlled cable is coded in two different environments. A control-oriented analytical Galerkin model is also derived. The sinusoidal eigenfunctions and eigenfrequencies of the cable equipped with the passive in-plane TMD are evaluated in closed form and are adopted in the Galerkin model. Numerical simulations are performed through the FEM model under spatial free oscillations. A harmonic analysis is also performed in the region of the primary resonance through the Galerkin model. The control action reveals to be capable to introduce a significant additional damping in the first two modes, in both free and harmonically forced oscillations. A high reduction of the first in-plane periodic modal amplitudes is observed in the vicinity of the primary resonance and in correspondence of the 1 : 2 resonance. The bifurcation of the first in-plane mode into a spatial oscillations is strongly reduced by the out-of-plane control action.

Detuning effects have also been considered in the harmonic analysis, by varying the sag and consequently the Irvine parameter of the uncontrolled cable. The proposed control strategy is seen to be rather robust to detuning effects, especially in the out-of-plane case. A small reduction in the in-plane control effectiveness is observed, as expected, with a progressive detuning of the TMD. Nevertheless, the sensitivity of the frequency response curve of the first in-plane mode to detuning effects is small and does not impair the overall control performance.

The variable inclination TMD is, therefore, an effective tool in reducing the spatial vibrations of steel cables, with considerable low cost. Some aspects are of particular interest about this topic and will be investigated with higher details in future developments. A comparison of different feedback control laws will be of great importance, also considering TMDs with variable features and nonlinear feedback control laws. Out-of-plane loading, such as harmonic excitation or wind action, is another worth research topic toward a better comprehension of the damping capability of the device. Finally, it will be of interest to path-follow both stable and unstable periodic solutions through an arclength approach implemented in bifurcation codes (as, for example, the software AUTO [37]).

Acknowledgements This paper was supported by the FAR of University of Pavia, coordinated by Professor Lucia Faravelli. The authors also acknowledge the support of the European Union, within the INTAS 2003-51-5547 contract, for which the first author served as coordinator.

Appendix

The hyperbolic eigenfunctions and eigenfrequencies of a cable with a passive in-plane TMD have been found by Cai et al. [29]. The sinusoidal eigenfunction are here derived to be used in the reduced Galerkin models.

The equation of motion of the free in-plane vibrations of a shallow cable of sag d and length l, with a passive TMD anchored at $x = x_0$, can be derived by neglecting the nonlinear terms and the external action in the in-plane equation of system (6) and by assuming that the axis of the TMD is parallel to the vertical direction ($\varepsilon = 0$):

$$Hv'' + \frac{8d}{l^2}h = \mu\ddot{v} + (kV + c\dot{V})\delta(x - x_0). \tag{18}$$

In (18), the hypothesis of small sag to span ratio is assumed and the static C_0 configuration is expressed by the parabola $Y(x) = \frac{\mu g l}{2H}(\frac{x^2}{l} - x)$. The term h in (18) is the tension increment due to the motion, which is given by the compatibility [8]:

$$h = -\frac{8ESd}{l^2 L_e}\int_0^l v\,dx \tag{19}$$

where $L_e = \int_0^l (\frac{ds}{dx})^3\,dx \cong [1 + 8(\frac{d}{l})^2]l$, ds being the infinitesimal curvilinear abscissa element defined along the cable.

The presence of the Dirac δ-function in (18) indicates that the control force produces a jump (first order discontinuity) in the spatial derivative v' at $x = x_0$. In particular, the following condition holds:

$$v'|_{x=x_0^+} - v'|_{x=x_0^-} = (kV + c\dot{V})/H \tag{20}$$

while the motion of the mass m of the TMD is regulated by the following equation:

$$\ddot{V} + \ddot{v}(x_0) + 2\xi_d\omega_d\dot{V} + \omega_d^2 V = 0 \tag{21}$$

where $\omega_d = (\frac{k}{m})^{1/2}$ and $\xi_d = \frac{c}{2m\omega_d}$. Let us assume a solution of the following type:

$$\begin{aligned} v(t) &= \mathrm{Re}\big[\tilde{v}(x)e^{\iota\omega t}\big], \\ h(t) &= \mathrm{Re}\big[\tilde{h}(x)e^{\iota\omega t}\big], \\ V(t) &= \mathrm{Re}\big[\tilde{V}(r)e^{\iota\omega t}\big] \end{aligned} \tag{22}$$

where ι is the imaginary unit and ω is a complex natural eigenfrequency. By inserting (22) into (18), one

can obtain the modal shapes of the cable $\tilde{v}_i(x)$ as functions of ω_i. It holds in particular:

$$\tilde{v}(x) = \tilde{v}(x_0)\frac{\sin(\beta x)}{\sin(\beta x_0)} + \frac{\tilde{h}}{H}\frac{8d}{(\beta L)^2} \times \left[\frac{\sin(\beta(x_0 - x)) + \sin(\beta x)}{\sin(\beta x_0)} - 1\right], \quad \text{if } x < x_0,$$
$$\tilde{v}(x) = \tilde{v}(x_0)\frac{\sin(\beta(l - x))}{\sin(\beta(l - x_0))} + \frac{\tilde{h}}{H}\frac{8d}{(\beta L)^2} \times \left[\frac{\sin(\beta(x - x_0)) + \sin(\beta(l - x))}{\sin(\beta(l - x_0))} - 1\right], \quad \text{if } x > x_0 \tag{23}$$

where $\beta_i = (\frac{\mu}{H})^{1/2}\omega_i$ and $\tilde{h}$ is defined in (22). The imaginary part of ω_i represents the modal damping introduced by the TMD, while its modulus is the natural angular frequency of the ith mode.

The link between the modal displacement $\tilde{v}(x_0)$ and the relative modal displacement $\tilde{V}$ between the mass of the TMD and the cable is also obtained as:

$$\tilde{V} = \frac{\omega^2}{\sqrt{(\omega_d^2 - \omega^2)^2 + (2\xi_d\omega_d\omega)^2}}\tilde{v}(x_0). \tag{24}$$

By using (23) into (19), one obtains:

$$\tilde{v}(x_0)\left[\frac{1 - \cos(\beta x_0)}{\sin(\beta x_0)} + \frac{1 - \cos(\beta(l - x_0))}{\sin(\beta(l - x_0))}\right] + \frac{\tilde{h}}{H}\frac{8d}{(\beta L)^2}\left[\frac{2 - 2\cos(\beta x_0)}{\sin(\beta x_0)} + \frac{2 - 2\cos(\beta(l - x_0))}{\sin(\beta(l - x_0))} - \beta l + \frac{\beta^3 l^3}{\lambda^2}\right] = 0 \tag{25}$$

where λ^2 is the nondimensional Irvine parameter of the cable. Finally, by inserting (23) and (24) into (20), the following relation holds true:

$$\tilde{v}(x_0)\left[\frac{\cos(\beta x_0)}{\sin(\beta x_0)} + \frac{\cos(\beta(l - x_0))}{\sin(\beta(l - x_0))} + \gamma\beta l\sqrt{\frac{\omega_d^4 + (2\xi_d\omega_d\beta l\frac{\omega_0}{\pi})^2}{(\omega_d^2 - (\beta l\frac{\omega_0}{\pi})^2)^2 + (2\xi_d\omega_d\beta l\frac{\omega_0}{\pi})^2}}\right] + \frac{\tilde{h}}{H}\frac{8d}{(\beta L)^2}\left[\frac{\cos(\beta x_0) - 1}{\sin(\beta x_0)} + \frac{\cos(\beta(l - x_0)) - 1}{\sin(\beta(l - x_0))}\right] = 0 \tag{26}$$

where $\omega_0 = \frac{\pi}{l}(\frac{H}{\mu})^{1/2}$ and $\gamma = \frac{m}{\mu l}$. Equations (25) and (26) give a nontrivial solution if the following condition is satisfied:

$$\sin\left(\frac{\beta l}{2}\right)\left[\sin\left(\frac{\beta l}{2}\right) - \cos\left(\frac{\beta l}{2}\right)\left(\frac{\beta l}{2} - \frac{4}{\lambda^2}\frac{\beta l^3}{2}\right)\right] = \gamma\beta l\sqrt{\frac{\omega_d^4 + (2\xi_d\omega_d\beta l\frac{\omega_0}{\pi})^2}{(\omega_d^2 - (\beta l\frac{\omega_0}{\pi})^2)^2 + (2\xi_d\omega_d\beta l\frac{\omega_0}{\pi})^2}} \times \sin\left(\frac{\beta x_0}{2}\right)\sin\left(\frac{\beta(l - x_0)}{2}\right) \times \left[\sin\left(\frac{\beta l}{2}\right) - \cos\left(\frac{\beta x_0}{2}\right)\cos\left(\frac{\beta(l - x_0)}{2}\right) \times \left(\frac{\beta l}{2} - \frac{4}{\lambda^2}\frac{\beta l^3}{2}\right)\right]. \tag{27}$$

The frequencies of a suspended cable without a control TMD device, calculated by Irvine's theory [8], are obtained from (27) when the right-hand side is zero. The presence of the TMD produces a change in the natural frequencies that tends quickly to zero as γ tends to zero. For a small value of the ratio γ, such a difference is negligible and the natural frequencies and modal shapes of the cable without the TMD could be assumed as a good approximation of the frequencies and modal shapes of the cable with the TMD.

References

1. Rega, G.: Nonlinear vibrations of suspended cables, part I: modeling and analysis. Appl. Mech. Rev. **57**, 443–478 (2004)
2. Rega, G.: Nonlinear vibrations of suspended cables, part II: deterministic phenomena. Appl. Mech. Rev. **57**, 479–514 (2004)
3. Larsen, J.W., Nielsen, S.R.K.: Non-linear stochastic response of a shallow cable. Int. J. Non-Linear Mech. **41**, 327–344 (2004)

4. Perkins, N.C.: Modal interactions in the non-linear response of elastic cables under parametric/external excitation. Int. J. Non-Linear Mech. **27**, 233–250 (1992)
5. Nayfeh, A.H., Arafat, H.N., Chin, C.M., Lacarbonara, W.: Multimode interactions in suspended cables. J. Vib. Control **8**, 337–387 (2002)
6. Benedettini, F., Rega, G., Alaggio, R.: Nonlinear oscillations of a four-degree of freedom model of a suspended cable under multiple internal resonance conditions. J. Sound Vib. **182**, 775–798 (1995)
7. Luongo, A., Rega, G., Vestroni, F.: Parametric analysis of large amplitude free vibrations of a suspended cable. Int. J. Solids Struct. **20**, 95–105 (1984)
8. Irvine, H.M., Caughey, T.K.: The linear theory of free vibrations of suspended cables. Proc. R. Soc. Lond. **341**, 299–315 (1974)
9. Arafat, H.N., Nayfeh, A.H.: Nonlinear responses of suspended cables to primary resonance excitations. J. Sound Vib. **266**, 325–354 (2003)
10. Desai, Y.M., Popplewell, N., Shah, A.H., Buragohain, D.N.: Geometric nonlinear analysis of cable supported structures. Comput. Struct. **29**(6), 1001–1006 (1988)
11. Desai, Y.M., Popplewell, N., Shah, A.H.: Finite element modeling of transmission line galloping. Comput. Struct. **57**, 407–420 (1995)
12. Gattulli, V., Martinelli, L., Perotti, F., Vestroni, F.: Nonlinear oscillations of cables under harmonic loading using analytical and finite element models. Comput. Methods Appl. Mech. Eng. **193**, 69–85 (2004)
13. Cluni, F.: Studio del comportamento dinamico dei cavi strutturali: modelli numerici e prove sperimentali. Dissertation, University of Perugia (2004) (in Italian)
14. Cluni, F., Gusella, V., Ubertini, F.: A parametric investigation of wind-induced cable fatigue. Eng. Struct. (2007). doi: 10.1016/j.engstruct.2007.02.010
15. Canbolat, H., Dawson, D., Rahn, C.D., Nagarkatti, S.: Adaptive boundary control of out-of-plane cable vibration. ASME J. Appl. Mech. **65**, 963–969 (1998)
16. Susumpow, T., Fujino, Y.: Active control of multimodal cable vibrations by axial support motion. Earthq. Eng. Struct. Dyn. **5**, 283–292 (1995)
17. Gattulli, V., Pasca, M., Vestroni, F.: Nonlinear oscillations of a nonresonant cable under in-plane excitation with a longitudinal control. Nonlinear Dyn. **14**(2), 139–156 (1997)
18. Alaggio, R., Gattulli, V., Potenza, F.: Experimental validation of longitudinal active control strategy for cable oscillations. In: Proceedings of the 9th Italian Conference on Wind Engineering (INVENTO), Pescara (2006)
19. Gattuli, V., Vestroni, F.: Nonlinear strategies for longitudinal control in the stabilization of an oscillating suspended cable. Dyn. Control **10**(4), 359–374 (2000)
20. Xu, Y.L., Yu, Z.: Non-linear vibration of cable-damper system, part I: formulation. J. Sound Vib. **225**, 447–463 (1999)
21. Xu, Y.L., Yu, Z.: Non-linear vibration of cable-damper system, part II: application and verification. J. Sound Vib. **225**, 465–481 (1999)
22. Zhou, Q., Nielsen, S.R.K., Qu, W.L.: Semi-active control of three-dimensional vibrations of an inclined sag cable with magnetorheological dampers. J. Sound Vib. **296**, 1–22 (2006)
23. Claren, R., Diana, G.: Vibrazioni dei conduttori. Energ. Elettr. **11**, 677–688 (1966) (in Italian)
24. Gattulli, V., Lepidi, M., Luongo, A.: Controllo con una massa accordata dell'instabilità aeroelastica di un cavo sospeso. In: Proceedings of the 16th Italian Conference on Theoretic and Applied Mechanics (AIMETA) (2003) (in Italian)
25. Pacheko, B.M., Fujino, Y., Sulekh, A.: Estimation curve for modal damping in stay cables with viscous dampers. ASCE J. Struct. Eng. **119**(6), 1961–1979 (1990)
26. Wu, W.J., Cai, C.S.: Experimental study of magnetorheological dampers and application to cable vibration control. J. Vib. Control **12**(1), 67–82 (2006)
27. Abdel-Rohman, M., Spencer, B.F.: Control of wind-induced nonlinear oscillations in suspended cables. Nonlinear Dyn. **37**, 341–355 (2004)
28. Markiewikz, M.: Optimum dynamic characteristics of stockbridge dampers for dead-end spans. J. Sound Vib. **188**, 243–256 (1995)
29. Cai, C.S., Wu, W.J., Shi, X.M.: Cable vibration reduction with a hung-on TMD system, part I: theoretical study. J. Vib. Control **12**(7), 801–814 (2006)
30. Cai, C.S., Wu, W.J., Shi, X.M.: Cable vibration reduction with a hung-on TMD system, part II: parametric study. J. Vib. Control **12**(8), 881–899 (2006)
31. Wu, W.J., Cai, C.S.: Cable vibration control with a magnetorheological fluid based tuned mass damper. In: Proceedings of the 10th Biennial ASCE Aerospace Division International Conference on Engineering, Construction, and Operations in Challenging Environments, League City/Houston, TX, USA, 5–8 March 2006
32. Casciati, F., Magonette, G., Marazzi, F.: Technology of Semiactive Devices and Applications in Vibration Mitigation. Wiley, Chichester (2006)
33. Casciati, F., Ubertini, F.: Control of cables nonlinear vibrations under turbulent wind action. In: Deodatis G., Spanos P. (eds.) Computational stochastic mechanics, 5th International Conference on Computational Stochastic Mechanics, Rodos, June 2006, pp. 169–178. Millpress, Rotterdam (2007)
34. ANSYS Inc.: ANSYS and CivilFEM 9.0 User Manual. Madrid (2005)
35. The Mathworks Inc.: Matlab and Simulink. Natick (2002)
36. Hilber, H.M., Hughes, T.J.R., Taylor, R.L.: Improved numerical dissipation for time integration algorithms in structural dynamics. Earthq. Eng. Struct. Dyn. **5**, 283–292 (1977)
37. Doedel, E.J., Paffenroth, R.C., Champneys, A.R., Fairgrieve, T.F., Kuznetsov, Y.A., Oldeman, B.E., Sandstede, B., Wang, X.: AUTO2000: continuation and bifurcation software for ordinary differential equations. Available online from http://indy.cs.concordia.ca/auto/